Free Radical Biology & Medicine 47 (2009) 1401–1407

Contents lists available at ScienceDirect

Free Radical Biology & Medicine

journal homepage: www.elsevier.com/locate/freeradbiomed

Original Contribution

Direct oxidation of boronates by peroxynitrite: Mechanism and implications in fluorescence imaging of peroxynitrite

Adam Sikora, Jacek Zielonka, Marcos Lopez, Joy Joseph, B. Kalyanaraman *

Department of Biophysics and Free Radical Research Center, Medical College of Wisconsin, Milwaukee, WI 53226, USA

ARTICLE INFO

Article history:
Received 8 July 2009
Revised 6 August 2009
Accepted 10 August 2009
Available online 14 August 2009

Keywords:
Boronic acids
Boronates
Peroxynitrite
Probes
Kinetics
Stopped flow
HPLC
Free radicals

ABSTRACT

In this study, we show that boronates, a class of synthetic organic compounds, react rapidly and stoichiometrically with peroxynitrite ($ONOO^-$) to form stable hydroxy derivatives as major products. Using a stopped-flow kinetic technique, we measured the second-order rate constants for the reaction with $ONOO^-$, hypochlorous acid (HOCl), and hydrogen peroxide (H_2O_2) and found that $ONOO^-$ reacts with 4-acetylphenylboronic acid nearly a million times ($k = 1.6 \times 10^6\ M^{-1}\ s^{-1}$) faster than does H_2O_2 ($k = 2.2\ M^{-1}\ s^{-1}$) and over 200 times faster than does HOCl ($k = 6.2 \times 10^3\ M^{-1}\ s^{-1}$). Nitric oxide and superoxide together, but not alone, oxidized boronates to the same phenolic products. Similar reaction profiles were obtained with other boronates. Results from this study may be helpful in developing a novel class of fluorescent probes for the detection and imaging of $ONOO^-$ formed in cellular and cell-free systems.

Peroxynitrite/peroxynitrous acid ($ONOO^-$/ONOOH), a potent oxidant and nitrating agent formed from the diffusion-controlled reaction between nitric oxide ($^{\bullet}NO$) and superoxide ($O_2^{\bullet-}$) anion, has been implicated as a key pathophysiological intermediate in various diseases, including acute and chronic inflammatory processes, ischemia–reperfusion, and neurodegenerative disorders [1–4]. Despite 2 decades of intense research, methodologies to directly detect and quantitate $ONOO^-$ in cellular and biological systems are still lacking [5,6]. As reiterated in recent reviews, the development of new probes and techniques for the direct detection of $ONOO^-$, a key reactive intermediate in redox biology, is essential for understanding the role of reactive nitrogen species in the biological milieu [7]. Most existing methods to detect $ONOO^-$ are based on the reaction of the hydroxyl radical ($^{\bullet}OH$) and the nitrogen dioxide radical ($^{\bullet}NO_2$), which form the radical pair cage, $^{\bullet}NO_2$ … $^{\bullet}OH$, with small organic molecules such as tyrosine, tryptophan, salicylic acid, and dihydrorhodamine [8–10]. Peroxynitrite reacts directly with thiols, methionine, ebselen, porphyrins, and carbonyl compounds [11–13]; yet these reactions have not been employed for $ONOO^-$ detection. The role of $ONOO^-$ has been questioned with regard to protein tyrosyl nitration [14,15]. Myeloperoxidase (MPO)/hydrogen peroxide (H_2O_2)-catalyzed oxidation of nitrite anion also could result in protein tyrosyl nitration [14,16]. Thus, probes that form a characteristic product by reacting rapidly and directly with $ONOO^-$, rather than with its radical intermediates, $^{\bullet}NO_2$ and $^{\bullet}OH$, are critically needed.

Toward this end, a new class of fluorescent probes containing a boronate structure has been developed for selective detection of H_2O_2 [17,18]. This assay was based on the conversion of weakly fluorescent arylboronates into strongly fluorescent phenolic products. Although the reaction of $^{\bullet}NO$ and $O_2^{\bullet-}$ with boronates was tested individually, the possibility of oxidation of boronates by $ONOO^-$ was not investigated [19,20]. In this study, we report that boronates (Fig. 1) react directly and rapidly with $ONOO^-$. This forms the corresponding hydroxyl derivatives, phenols, as major products. The rate constant determined for this reaction is several orders of magnitude greater than for H_2O_2 or hypochlorous acid (HOCl). Potential implications for imaging of $ONOO^-$ in cells using boronate-containing fluorescence probes are discussed.

Materials and methods

Materials

Phenylalanine boronic acid (FBA) was obtained from Ryscor Science, and the other boronic compounds were from Boron Mole-

Abbreviations: CAT, catalase; DTPA, diethylenetriaminepentaacetic acid; EtBA, ethylboronic acid; FBA, 4-phenylalanine boronic acid; $GS^{\bullet}$, glutathiyl radical; GSH, glutathione; HCO_3^-, bicarbonate anion; HOO^-, hydroperoxide anion; MPO, myeloperoxidase; $^{\bullet}NO$, nitric oxide; $^{\bullet}NO_2$, nitrogen dioxide radical; NO_2^-, nitrite anion; $O_2^{\bullet-}$, superoxide radical anion; OCl^-, hypochlorite anion; $^{\bullet}OH$, hydroxyl radical; $ONOO^-$, peroxynitrite; PAPA-NONOate, (*Z*)-1-[*N*-(3-aminopropyl)-*N*-(*n*-propyl)amino]diazen-1-ium-1,2-diolate; PBA, 4-acetylphenylboronic acid; PBE, 4-acetylphenylboronic acid pinacol ester; SOD, superoxide dismutase; X, xanthine; XO, xanthine oxidase.

* Corresponding author. Fax: +1 414 456 6512.
E-mail address: balarama@mcw.edu (B. Kalyanaraman).

0891-5849/$ – see front matter © 2009 Elsevier Inc. All rights reserved.
doi:10.1016/j.freeradbiomed.2009.08.006

cular. Xanthine oxidase (XO) and superoxide dismutase (SOD) were from Roche Diagnostics, CAT was from Boehringer Mannheim, MPO was from Calbiochem, and all other reagents (of highest purity available) were from Sigma. All solutions were prepared using deionized water (Millipore Milli-Q system). $ONOO^-$ was prepared by reacting nitrite with H_2O_2, according to the published procedure [21]. The concentration of $ONOO^-$ in alkaline aqueous solutions (pH>12) was determined by measuring the absorbance at 302 nm ($\varepsilon = 1670\ M^{-1}\ cm^{-1}$).

Determination of $O_2^{\cdot-}$ and $^{\cdot}NO$ fluxes

$^{\cdot}NO$ fluxes were determined from the measured rate of the decomposition of PAPA-NONOate by following the decrease in its characteristic absorbance at 250 nm ($\varepsilon = 8\times10^3\ M^{-1}\ cm^{-1}$). This rate was multiplied by a factor of 2 to get the rate of $^{\cdot}NO$ release (assuming that two molecules of $^{\cdot}NO$ are released from one molecule of PAPA-NONOate). Superoxide flux was determined by monitoring the cytochrome *c* reduction following the increase in absorbance at 550 nm (using an extinction coefficient of $2.1\times10^4\ M^{-1}\ cm^{-1}$).

Oxidation of boronic compounds induced by $ONOO^-$, H_2O_2, HOCl, $O_2^{\cdot-}$, and MPO/H_2O_2

Typically, boronic acids and esters (100 μM) were incubated with MPO (15 nM), H_2O_2 (50 μM), and $NaNO_2$ (500 μM) or NaCl (0.15 M) in a phosphate buffer (100 mM, pH 7.4) containing DTPA (10 μM) at room temperature for 30 min. Reactions were terminated by adding CAT (100 U/ml) and directly analyzed by HPLC. In other experiments, boronic compounds (100 μM) were incubated with XO, xanthine (X) (200 μM), and PAPA-NONOate (30 μM) in a phosphate buffer (100 mM, pH 7.4) solution containing DTPA (10 μM) at room temperature for 15 min. The reaction mixtures contained CAT (100 U/ml) and/or SOD enzyme (0.5 mg/ml). Finally, in some experiments, boronic compounds (100 μM) were rapidly mixed with $ONOO^-$ (10–250 μM), hypochlorous acid (10–250 μM), or H_2O_2 (10–250 μM) in a phosphate buffer (100 mM, pH 7.4). With $ONOO^-$ and HOCl, reaction mixtures were incubated at room temperature for 10 min and then analyzed by HPLC. With H_2O_2, samples were incubated for several hours before HPLC analysis. To investigate the effect of carbon dioxide (CO_2) on the yield of the phenolic product of the reaction of boronates with $ONOO^-$, we carried out the reaction in the presence of sodium bicarbonate ($NaHCO_3$). Bicarbonate anion is known to exist at neutral pH in the equilibrium with CO_2 and, based on the dissociation constant of carbonic acid ($pK_a = 6.35$), we calculated the concentration of CO_2 at pH 7.4 to be 2.2 mM in equilibrium with 25 mM HCO_3^- anions. To ensure the solutions reached this equilibrium, peroxynitrite was added 10–20 min after the solutions were prepared.

HPLC and UV–Vis analyses of oxidation products

HPLC experiments were performed using an Agilent 1100 system. For detecting boronic compounds and their oxidation products, typically 10 μl of sample was injected into the HPLC system equipped with a C18 column (Alltech, Kromasil, 250×4.6 mm, 5 μm, 80 Å) that was equilibrated with 5% CH_3CN [containing 0.1% (v/v) trifluoroacetic acid (TFA)] in 0.1% TFA aqueous solution. Compounds were eluted during a linear increase in the acetonitrile fraction from 5 to 100% over 60 min (using a flow rate of 0.5 ml/min). For the quantification of FBA and the products of its reaction with $ONOO^-$, typically 50 μl of sample was injected into the HPLC system equipped with a Synergi Hydro-RP column (Phenomenex, 250×4.6 mm, 4 mm) that was equilibrated with an aqueous solution of TFA (0.1%). Over the first 20 min after injection, the CH_3CN fraction was increased from 0 to 5%, and from 5 to 20% over the next 15 min. The flow rate was set at 1 ml/min. The UV–Vis absorption spectra were collected using an Agilent 8453 spectrophotometer.

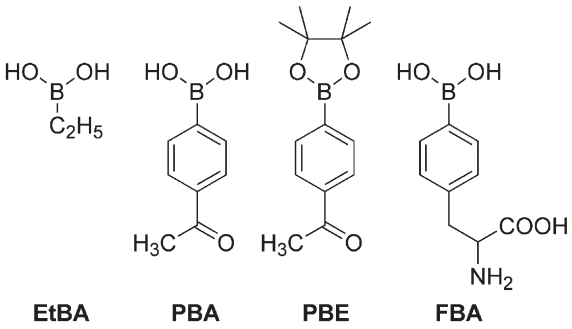

Fig. 1. Chemical structures of boronates used in this study.

Stopped-flow measurements

Stopped-flow kinetic experiments were performed on an Applied Photophysics 18MX stopped-flow spectrophotometer equipped with a photomultiplier for absorption measurements [22]. The thermostated cell (25°C) with a 10-mm optical pathway was used for kinetic measurements. Typically, reactions were performed under pseudo-first-order conditions (greater than 10-fold excess boronate over $ONOO^-$ at boronate concentrations ranging from 100 μM to 1 mM).

Kinetic analysis

The kinetic traces were fitted to a single-exponential function corresponding to the first-order kinetics. Results from the fitting of at least three kinetic traces were averaged to obtain the first-order rate constant. From the slopes of the plots of the observed first-order rate constants versus the concentration of the reactant, the second-order rate constants were obtained.

Results

Kinetics of oxidation of boronates

The reaction kinetics for boronate oxidation by $ONOO^-$, HOCl, and H_2O_2 were investigated under pseudo-first-order conditions, using an excess of either boronate in the case $ONOO^-$ or the oxidants HOCl and H_2O_2. The rate constants for the reactions of selected aromatic and aliphatic boronic compounds are shown in Table 1. Remarkably, $ONOO^-$ reacts with boronates as fast as it reacts with ebselen. Fig. 2 shows the comparative kinetic traces of $ONOO^-$, H_2O_2, and HOCl with 4-acetylphenylboronic pinacolate ester (PBE). As shown, the reaction of H_2O_2 with boronates is much slower (over a period of hours under the experimental conditions used) compared with $ONOO^-$, which takes place at a millisecond time scale. Reaction between boronates and HOCl occurred over several seconds. This is one of the fastest reactions of $ONOO^-$ with low-molecular-weight organic molecules. The rate constant between aliphatic boronate (ethylboronic acid, EtBA) and $ONOO^-$, obtained by monitoring the decomposition of $ONOO^-$ at 302 nm [21] (Fig. 3), was an order of magnitude lower than for aromatic analogs (Table 1).

Quantitation of products of boronate oxidation: stoichiometric analyses

The oxidation of 4-acetylphenylboronic ester by $ONOO^-$, H_2O_2, and HOCl was monitored by following the substrate consumption and the formation of corresponding 4′-hydroxyacetophenone using the HPLC technique (Fig. 4). As shown in Fig. 4A, PBE eluted at 21.9 min. With increasing concentration of $ONOO^-$, the intensity due to the PBE

Table 1
The apparent second-order rate constants of the reaction of boronates with $ONOO^-$, HOCl, and H_2O_2 at pH 7.4.

Boronate	Second-order rate constant, k ($M^{-1}\,s^{-1}$)		
	Peroxynitrite	Hypochlorous acid	Hydrogen peroxide
EtBA	$(2.8\pm0.2)\times10^5$	$(1.2\pm0.2)\times10^4$	–[a]
PBA	$(1.6\pm0.3)\times10^6$	$(6.2\pm0.3)\times10^3$	2.2 ± 0.1
PBE	$(1.2\pm0.3)\times10^6$	$(5.7\pm0.3)\times10^3$	2.2 ± 0.1
FBA	$(1.4\pm0.3)\times10^6$	$(2.7\pm0.3)\times10^4$	2.5 ± 0.1

[a] Not measured.

peak decreased, and another peak eluting at 23.2 min (marked by a downward arrow) appeared. This new peak coincided with that of the 4′-hydroxyacetophenone. With further increase in $ONOO^-$ (250 μM), another peak eluting at 32 min appeared. This is also formed from 4′-hydroxyacetophenone and $ONOO^-$ (marked by an asterisk). This peak has been assigned to the nitrated phenol, as it coeluted with the authentic standard of 3′-nitro-4′-hydroxyacetophenone.

Fig. 4B shows the HPLC chromatograms of reaction mixtures of PBE with HOCl. With increasing HOCl concentration, PBE was oxidized to the corresponding phenol (marked by a downward arrow). In the presence of increasing HOCl concentration, an additional peak, attributable to the chlorinated product (marked by an asterisk), was detected. Addition of taurine to the reaction mixture inhibited the reaction, indicating that HOCl, but not chloramine formed in the reaction of HOCl with taurine, is able to convert boronic compounds into phenols. Fig. 4C shows the HPLC chromatograms of the reaction mixtures containing PBE and H_2O_2. Similar to $ONOO^-$ and HOCl, H_2O_2 oxidized PBE to 4′-hydroxyacetophenone. However, in contrast to $ONOO^-$ and HOCl, with increasing concentrations of H_2O_2 there was no further oxidation of the phenol formed during the reaction. Fig. 5 shows the substrate depletion and product formation during titration of PBE with $ONOO^-$, HOCl, and H_2O_2. It is evident that PBE reacts with all three oxidants stoichiometrically, with one molecule of the boronate consumed per molecule of the oxidant. However, whereas in the case of HOCl and H_2O_2, the maximal yield of the phenol was close to 100%, the yield obtained with $ONOO^-$ reached 80–85%. Increasing the concentration of $ONOO^-$ decreased the yield of phenol. Similar results were obtained with FBA (Fig. 6). Tyrosine was formed as a major product during oxidation of FBA by $ONOO^-$, and nitrotyrosine and dityrosine were formed even in the presence of excess FBA, when the reaction of $ONOO^-$ with the corresponding phenol (i.e., tyrosine) is not very probable. This indicates that a small fraction (<20%) of the adduct of $ONOO^-$ to the boronic compound decays via free radical pathways. The exact nature of the reactions occurring during the decomposition of the adduct is currently under investigation.

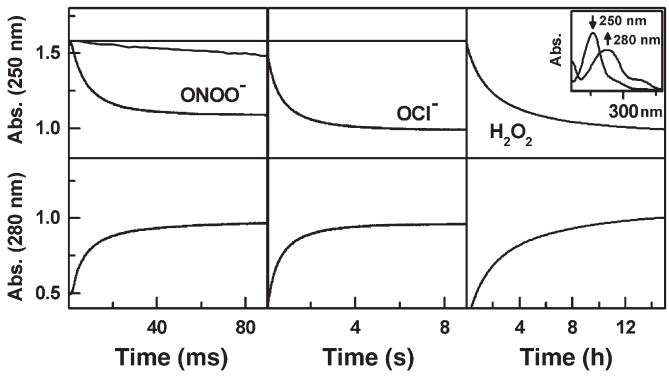

Fig. 2. Kinetics of the phenyl boronic ester reactions with $ONOO^-$, hypochlorite, and H_2O_2. The decay kinetics of PBE were monitored at 250 nm and formation of 4′-hydroxyacetophenone was monitored at 280 nm. Incubations contained 100 μM PBE and 100 μM oxidant (after mixing) in phosphate buffer (pH 7.4, 100 mM) containing DTPA (10 μM). Measurements were made at room temperature. (Inset) The absorption spectra of PBE ($\lambda_{max}=250$ nm) and 4′-hydroxyacetophenone ($\lambda_{max}=280$ nm).

Oxidation of boronates in X/XO and PAPA-NONOate systems

The oxidation of PBE was investigated in the presence of $O_2^{\cdot-}$ and $^{\cdot}NO$. To this end, PBE (100 μM) was incubated with X (200 μM) and XO (10 mU/ml) in phosphate buffer (100 mM, pH 7.4) containing DTPA (10 μM) for 15 min at room temperature, and the products were analyzed by HPLC (Fig. 7, left). In parallel, similar incubations were performed but in the presence of a $^{\cdot}NO$ donor, PAPA-NONOate (100 μM), and the products were analyzed by HPLC (Fig. 7, right). In the absence of PAPA-NONOate, there was a modest conversion of PBE to 4′-hydroxyacetophenone, which was sensitive to CAT, but not to the SOD addition (Fig. 7, left), indicating that H_2O_2, but not $O_2^{\cdot-}$, was responsible for the oxidation of PBE. In contrast, the addition of PAPA-NONOate to the incubation mixtures containing PBE and X/XO significantly enhanced the formation of 4′-hydroxyacetophenone, which was inhibited (=50%) in the presence of high concentrations of SOD but not of CAT (Fig. 7, right). This suggests that $ONOO^-$ formed from $^{\cdot}NO$ and $O_2^{\cdot-}$ is responsible for oxidation of PBE to the corresponding phenol. In the X/XO/PAPA-NONOate system (generating equal fluxes of $^{\cdot}NO$ and $O_2^{\cdot-}$) the amount of PBE consumed was nearly equal to the amount of $ONOO^-$ that was expected to be produced during the incubation, and the 4′-hydroxyacetophenone was formed at the 90% yield (compared to the amount of PBE consumed).

Glutathione (GSH) and CO_2 effects on boronate oxidation by $ONOO^-$

As $ONOO^-$-dependent reactions are often altered in the presence of biologically relevant reductants (e.g., GSH) and HCO_3^- [23–25], we investigated the effects of varying the levels of GSH and HCO_3^- on the extent of $ONOO^-$-mediated oxidation of boronate, PBE. Fig. 8A shows the effect of increasing concentrations of GSH on 4′-hydroxyacetophenone formation in incubation mixtures containing PBE in phosphate buffer (100 mM, pH 7.4) and DTPA (10 μM). In the presence of relatively low concentrations of GSH (1 mM or less), there was enhanced formation of 4′-hydroxyacetophenone. With increasing GSH concentration, the yield of the phenolic product decreased; however, even in the presence of 6–7 mM GSH, $ONOO^-$ reacted with PBE, forming 4′-hydroxyacetophenone, although the yield gradually decreased. The decrease in the yield of 4′-hydroxyacetophenone may be explained in terms of the competition between PBE and GSH for $ONOO^-$. The reason for an increase in phenol yield at lower concentrations of GSH is less clear at present. When incubations were carried out in N_2-purged solutions, this increase in product formation (at low GSH) was largely abolished (Fig. 8B). This finding

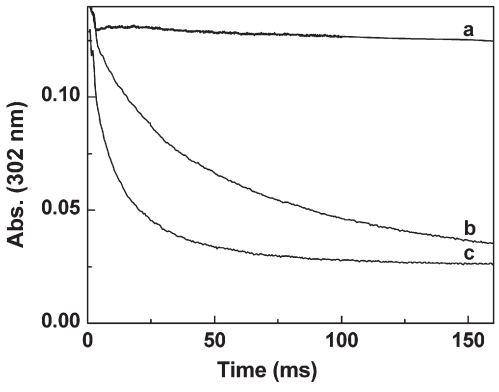

Fig. 3. Decay kinetics of $ONOO^-$ at 25°C in phosphate buffer (pH 7.4, 250 mM) (a) in the absence of boronates, (b) in the presence of EtBA (100 μM), and (c) in the presence of PBA (100 μM).

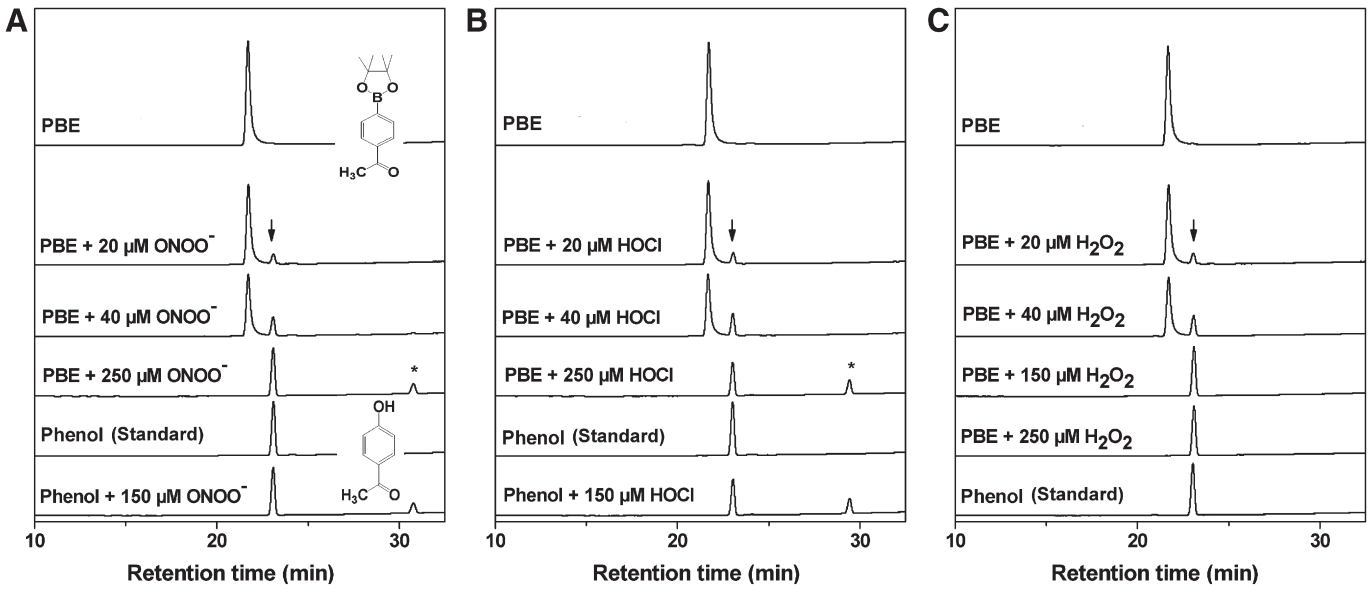

Fig. 4. HPLC analyses of products formed from the reactions between PBE and (A) $ONOO^-$, (B) HOCl, and (C) H_2O_2. Incubation mixtures consisted of 100 μM PBE in phosphate buffer (pH 7.4, 100 mM) containing DTPA (10 μM) and oxidants at the indicated concentrations. PBE and the corresponding phenol, 4′-hydroxyacetophenone, were detected using the HPLC/UV detection at 250 nm. Asterisks indicate nitrated and chlorinated tyrosyl products. In the case of the HOCl experiments, DTPA was omitted.

suggests that an oxidant(s) derived from the adduct of $ONOO^-$ with PBE can react with GSH and form a reactive intermediate in the presence of oxygen that may increase the yield of phenol.

HCO_3^- is another ubiquitous component in cells. As $ONOO^-$ reacts with CO_2, forming an intermediate, nitrosoperoxycarbonate anion ($ONOOCO_2^-$; with a half-life <1 ms), that decomposes to $^{\cdot}NO_2$ and carbonate radical anion ($CO_3^{\cdot-}$) [26,27], the effects of varying the concentrations of HCO_3^- and GSH on boronate oxidation were investigated. There was a concentration-dependent decrease in the extent of PBE oxidation to 4′-hydroxyacetophenone by $ONOO^-$ in the presence of HCO_3^- (Fig. 8C). The addition of GSH (500 μM) to the above incubation mixture increased the yield of 4′-hydroxyacetophenone. This increase was again dependent on the presence of oxygen, indicating that GSH-derived oxidation products may induce additional product formation from boronate. Overall, these results suggest that, even in the presence of GSH and HCO_3^-, $ONOO^-$ can convert boronates into corresponding phenols.

Oxidation of boronates by the MPO/H_2O_2 system

To investigate whether other reactive nitrogen species (e.g., $^{\cdot}NO_2$) oxidize boronate in the same way as does $ONOO^-$, we used the MPO and H_2O_2 system. PBE was incubated with MPO, H_2O_2, and nitrite anion (NO_2^-) in phosphate buffer (50 mM, pH 7.4) containing DTPA (10 μM). Unlike $ONOO^-$, the oxidant ($^{\cdot}NO_2$) generated from MPO, H_2O_2, and NO_2^- did not increase 4′-hydroxyacetophenone formation. The yield of the phenolic product was, however, enhanced in the presence of GSH (Fig. 9). This is tentatively attributed to oxidation of boronate by GSH/$^{\cdot}NO_2$/O_2-derived oxidants. Although $^{\cdot}NO_2$ by itself is not responsible for oxidation of PBE to the corresponding phenol, GSH accelerates the conversion of PBE to 4′-hydroxyacetophenone. In the presence of chloride anion, there was increased formation of phenol due to HOCl-mediated oxidation of boronate.

Discussion

Here we have shown that $ONOO^-$ reacts directly with boronic compounds yielding the corresponding hydroxyl derivatives (phenols or alcohols) as final products. Compared to reactivity between $ONOO^-$ and other small organic molecules, the bimolecular rate constant ($k = 10^6$ M^{-1} s^{-1}) measured for the reaction between $ONOO^-$ and boronates is very high. This high reactivity of boronic compounds toward $ONOO^-$, compared with other oxidants, makes them attractive candidates as potential traps and fluorescent probes

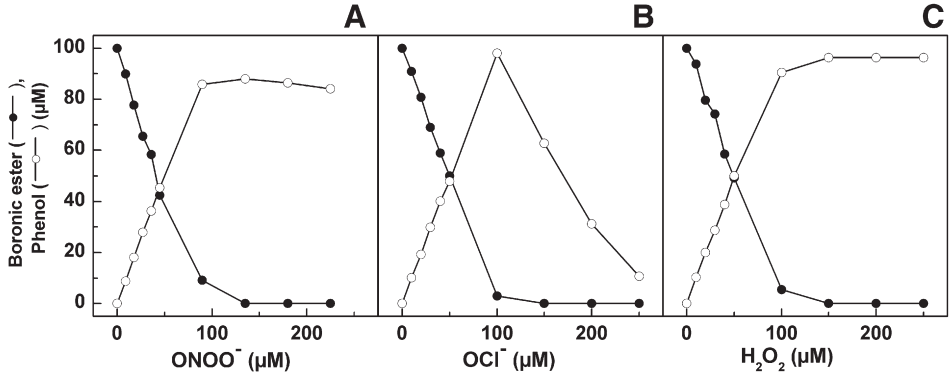

Fig. 5. Relationship between substrate depletion and product formation from reaction of the boronate with oxidants. (A–C) Experimental conditions were essentially the same as for Fig. 3. After a 15-min ($ONOO^-$, HOCl) or 24-h (H_2O_2) incubation period, the reaction mixtures were analyzed using the HPLC/UV method. PBE was detected at 250 nm and 4′-hydroxyacetophenone at 280 nm.

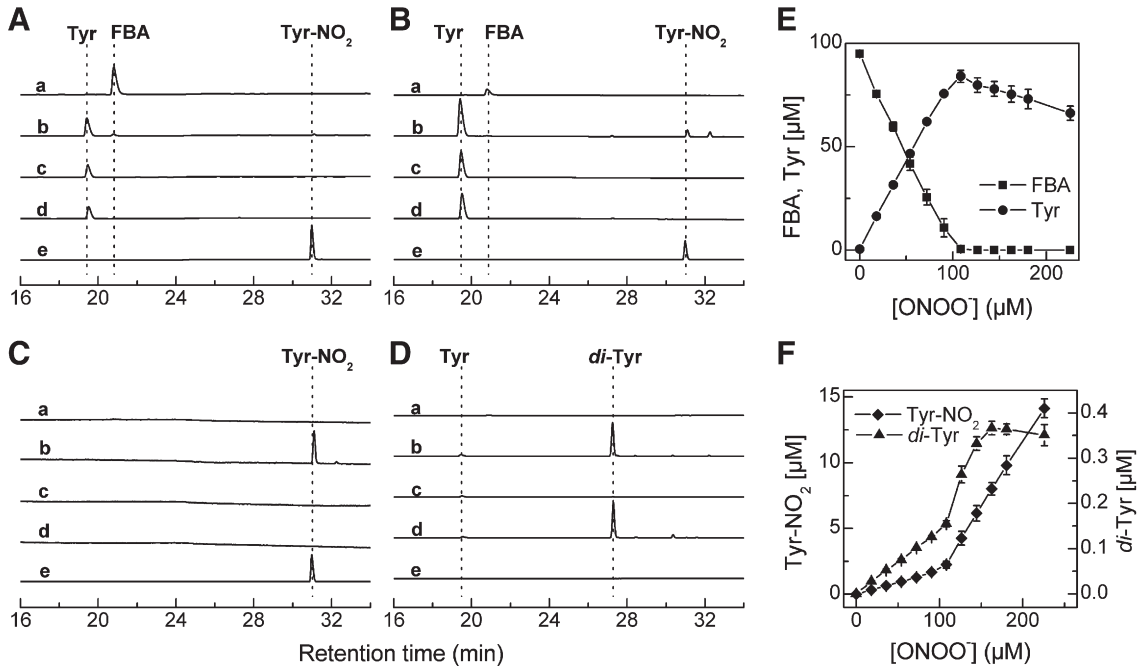

Fig. 6. HPLC chromatograms of the reaction between FBA and $ONOO^-$. (A–C) Absorption traces recorded at (A) 220 , (B) 280, and (C) 350 nm. (D) Fluorescence traces (excitation at 284 nm, emission at 410 nm). (Traces a) FBA (250 μM); (b) FBA (250 μM) + $ONOO^-$ (200 μM); (c) Tyr (100 μM); (d) Tyr (100 μM) + horseradish peroxidase (10 nM) + H_2O_2 (100 μM); (e) Tyr-NO_2 (100 μM). All samples were incubated for 15 min at room temperature in aqueous solution containing phosphate buffer (0.1 M, pH 7.4) and DTPA (10 μM). To fit the scale, traces e have been scaled down by factors of 0.1 (B) and 0.03 (C). (E and F) The dependence of the phenylalanine boronate and nitrotyrosine concentrations in the reaction mixtures on the amount of $ONOO^-$ added to the solution of FBA (100 μM).

for cellular imaging of $ONOO^-$. From product analyses and substrate consumption studies, we conclude that boronates react with $ONOO^-$ at a 1:1 stoichiometry, yielding the corresponding phenol as a major product (80–85%) and possibly free radical intermediates and radical-derived products as minor products (<20%). We propose a reaction scheme in which the initial reaction occurs with the formation of the $ONOO^-$ adduct to the boronic compound, which subsequently decomposes predominantly via a nonradical pathway forming the phenolic product (Fig. 10). HOCl and H_2O_2 react stoichiometrically

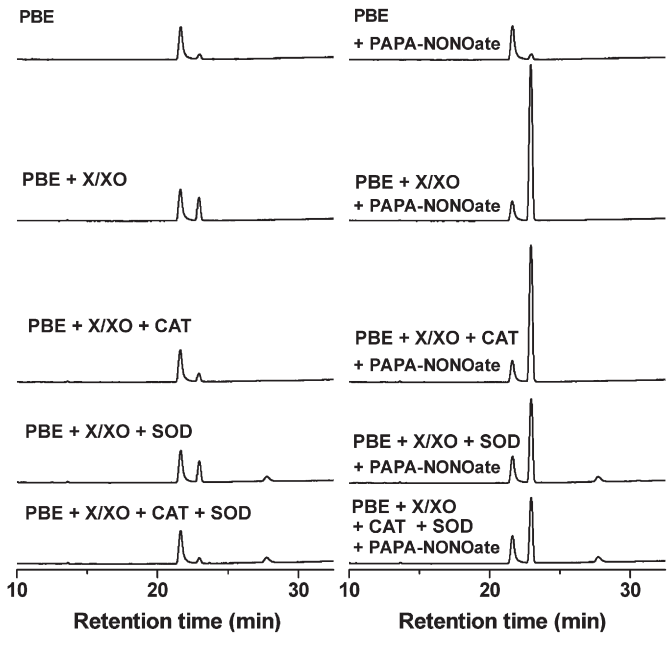

Fig. 7. HPLC analyses of products formed from X/XO/PAPA-NONOate-dependent oxidation of PBE. Incubation mixtures included 100 μM PBE and X (200 μM)/XO in phosphate buffer (pH 7.4, 100 mM) containing 10 μM DTPA, in the presence or absence of PAPA-NONOate (100 μM). After a 15-min incubation at room temperature, the products were analyzed as described for Fig. 3. Where indicated, CAT (100 U/ml) and SOD (0.5 mg/ml) were added. $O_2^{\cdot-}$ and $^{\cdot}NO$ fluxes (2.6 μM/min each) were determined as described under Materials and methods. PBE and 4′-hydroxyacetophenone were detected at 280 nm.

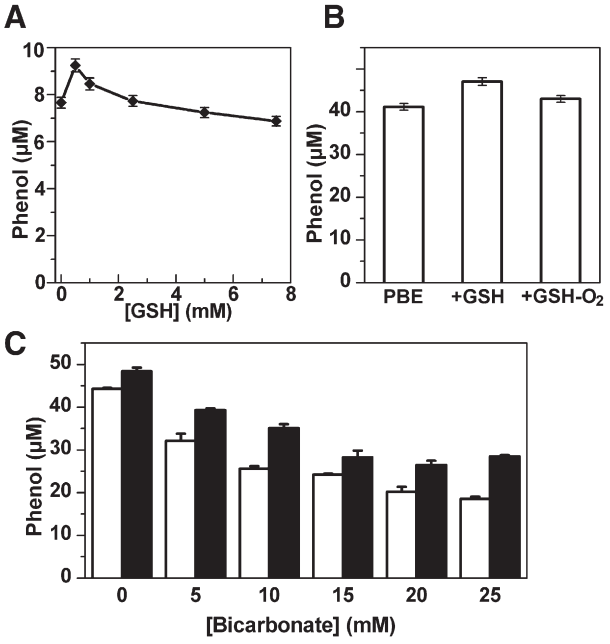

Fig. 8. The effects of glutathione and HCO_3^- on boronate oxidation by $ONOO^-$. (A) Incubation mixtures contained PBE (50 μM), $ONOO^-$ (10 μM), and GSH at the concentrations indicated in phosphate buffer (pH 7.4, 100 mM) containing DTPA (10 μM). (B) Relative concentrations of 4′-hydroxyacetophenone formed in incubation mixtures containing PBE (100 μM), GSH (500 μM), and $ONOO^-$ (50 μM, slow infusion 10 μM/min) in phosphate buffer (pH 7.4, 100 mM) containing DTPA (10 μM). The product was measured 15 min after the addition of $ONOO^-$. (C) PBE (100 μM) was mixed with $ONOO^-$ (50 μM) in a phosphate buffer (pH 7.4, 100 mM) containing DTPA (10 μM) and HCO_3^- (open bars) or GSH (500 μM) and HCO_3^- (solid bars).

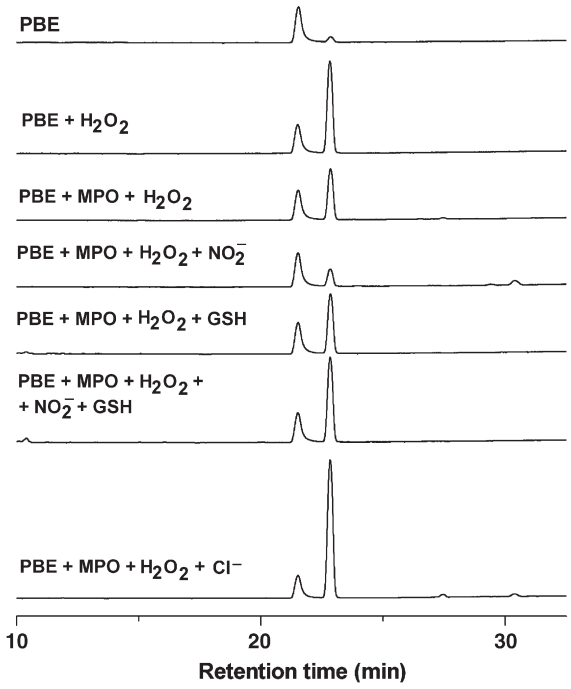

Fig. 9. HPLC analyses of products formed during MPO/H_2O_2-mediated oxidation of boronates. Incubation mixtures contained PBE (100 μM), MPO (15 nM), H_2O_2 (50 μM), and other agents, NO_2^- (500 μM), NaCl (0.15 M), or GSH (500 μM), as indicated, in phosphate buffer (pH 7.4, 100 mM) with DTPA (10 μM). Reaction was initiated by the addition of H_2O_2. Products were measured 15 min after addition of H_2O_2.

with boronates yielding the corresponding phenol (Fig. 10), although at much slower rates compared to $ONOO^-$ (Table 1).

Studies with X/XO and NONOates indicate that neither $O_2^{\cdot-}$ nor $^{\cdot}NO$ reacts with boronates. We verified that nitrogen dioxide alone does not convert the boronic compounds into phenols. $ONOO^-$-mediated oxidation of PBE to 4′-hydroxyacetophenone was enhanced in the presence of low concentrations of GSH and moderately attenuated at high concentrations of GSH (Fig. 8). The GSH-mediated increase in 4′-hydroxyacetophenone formation was oxygen-dependent and CAT-independent. This suggests that the reactive species derived from glutathiyl radical and molecular oxygen, but not glutathiyl radical per se, can oxidize boronic compounds to the corresponding phenols. The lack of the CAT effect also excludes the possible involvement of H_2O_2 that could be produced via the reaction of glutathiyl radical ($GS^{\cdot}$) radical with glutathiolate anion (GS^-), with formation of glutathione disulfide radical anion ($GSSG^{\cdot-}$) and subsequent oxygen reduction leading to $O_2^{\cdot-}$ radical anion that dismutates to H_2O_2. Enhanced production of 4′-hydroxyacetophenone from PBE was also observed in incubations containing HCO_3^- and GSH, possibly due to formation of $GS^{\cdot}$ radical.

Boronates react with $ONOO^-$ nearly a million times faster than with H_2O_2. The boronic acid group, wherein the boron atom is sp^2-hybridized, is a very strong electrophile, and its reaction with a powerful nucleophile, $ONOO^-$, is energetically favored. Nearly 4 decades ago, Keith and Powell reported that the decomposition of $ONOO^-$ was increased in borate buffer, which was attributed to a transperoxidation reaction between $ONOO^-$ and borate, forming a peroxyborate intermediate [28]. Recently, it was shown that peroxymonophosphate reacts with boronates much faster than does H_2O_2 [29]. In the case of oxidants studied in this paper, reaction time scales ranged from milliseconds (for $ONOO^-$) to seconds (for OCl^-) and hours (for hydroperoxide anion, HOO^-) (Fig. 1, Table 1). At physiological pH (≈7.4), the percentage of HOO^- is 0.005%, compared to $ONOO^-$ (83%) and OCl^- (46%). This is consistent with the pK_a's of H_2O_2 (11.7), ONOOH (6.7), and HOCl (7.47). This may partially explain the differences in the observed second-order rate constants for these species with boronates. Although HOCl reacts with boronates a hundred to a thousand times slower than $ONOO^-$, this reaction may still be viable, because of its increased chemical stability. However, owing to more rapid electrophilic reactions of HOCl with endogenous amines and thiols, it is rather unlikely that the boronic compounds can effectively compete for HOCl in the cellular systems. Moreover, the specific scavengers of HOCl (e.g., taurine) can be used to identify the nature of intracellular oxidant responsible for boronate oxidation.

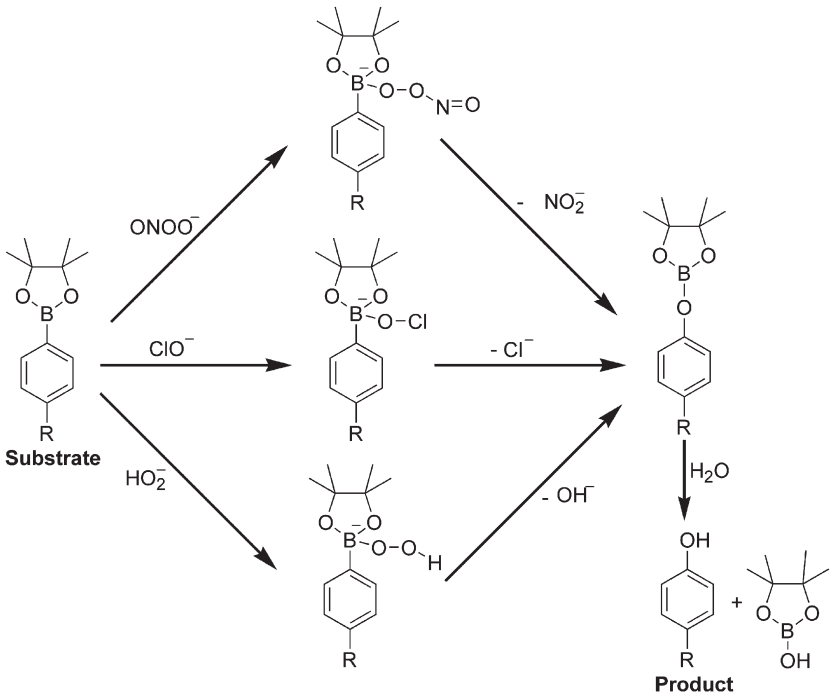

Fig. 10. Proposed mechanism of oxidation of boronates by $ONOO^-$, HOCl, and H_2O_2.

The conversion of phenylboronic esters by $ONOO^-$, HOCl, and H_2O_2 to the corresponding phenolic product is shown in Fig. 10. The initial step of the reaction involves a bimolecular collision between the electrophilic boronate and the nucleophilic anion ($ONOO^-$, OCl^-, HOO^-). With H_2O_2 and HOCl, nearly a 100% conversion of the boronate to the corresponding phenolic product occurs (Fig. 5). Additional products were not formed with H_2O_2; however, as shown in Fig. 5, higher concentrations of HOCl caused a rapid decrease in the levels of phenolic product. This is attributed to formation of the corresponding chlorinated phenol. In the case of $ONOO^-$, the yield of the phenolic product was about 85% (Fig. 5). The published reports on the reaction between $ONOO^-$ and carbonyl compounds and carbon dioxide indicate that the adducts formed decompose by a nonradical and radical pathway [13,30]. It is likely that a similar radical-mediated minor decomposition pathway occurs for the boronate/$ONOO^-$ adduct. Formation of dityrosyl-type products strongly implicates a role for radical-mediated decomposition. We are currently investigating the radical-mediated minor pathway in detail. We believe that the proposed reaction pathway between boronates and $ONOO^-$, OCl^-, and HOO^- is quite general and should be applicable to many other boronates. The rapid direct reaction between arylboronates and $ONOO^-$, compared to H_2O_2, coupled with a nearly stoichiometric conversion of the adduct into phenolic product, makes boronate-based fluorescent probes ideal candidates for cellular imaging of $ONOO^-$. Potential boronate-based fluorescence probes, some of which have already been reported in the literature [20,31,32], are shown in Supplementary Fig. S1. It is likely that fluorescein-based boronates will be eminently suitable for detection and imaging of cellular $ONOO^-$ owing to their high fluorescent quantum yields and suitable excitation/emission characteristics.

In conclusion, we have shown that several oxidants ($ONOO^-$, HOCl, H_2O_2) react stoichiometrically at different rates with boronates, a class of organic compounds, which can be incorporated into several fluorescent probes, to generate the corresponding phenols. This study opens up new possibilities for quantitative detection and inhibition of $ONOO^-$ in cells by using boronate-containing probes in biological systems.

Acknowledgment

This work was performed with the help of a grant funded by the NHLBI (HL063119).

Appendix A. Supplementary data

Supplementary data associated with this article can be found in, the online version, at doi:10.1016/j.freeradbiomed.2009.08.006.

References

[1] Beckman, J. S.; Beckman, T. W.; Chen, J.; Marshall, P. A.; Freeman, B. A. Apparent hydroxyl radical production by peroxynitrite: implications for endothelial injury from nitric oxide and superoxide. *Proc. Natl. Acad. Sci. USA* **87:**1620–1624; 1990.
[2] Pacher, P.; Beckman, J. S.; Liaudet, L. Nitric oxide and peroxynitrite in health and disease. *Physiol. Rev.* **87:**315–424; 2007.
[3] Radi, R. Nitric oxide, oxidants, and protein tyrosine nitration. *Proc. Natl. Acad. Sci. USA* **101:**4003–4008; 2004.
[4] Schopfer, F. J.; Baker, P. R.; Freeman, B. A. NO-dependent protein nitration: a cell signaling event or an oxidative inflammatory response? *Trends Biochem. Sci.* **28:** 646–654; 2003.
[5] Ferrer-Sueta, G.; Radi, R. Chemical biology of peroxynitrite: kinetics, diffusion, and radicals. *ACS Chem. Biol.* **4:**161–177; 2009.
[6] Szabo, C.; Ischiropoulos, H.; Radi, R. Peroxynitrite: biochemistry, pathophysiology and development of therapeutics. *Nat. Rev. Drug Discovery* **6:**662–680; 2007.
[7] Radi, R. Peroxynitrite and reactive nitrogen species: the contribution of ABB in two decades of research. *Arch. Biochem. Biophys.* **484:**111–113; 2009.
[8] Augusto, O.; Gatti, R. M.; Radi, R. Spin-trapping studies of peroxynitrite decomposition and of 3-morpholinosydnonimine *N*-ethylcarbamide autooxidation: direct evidence for metal-independent formation of free radical intermediates. *Arch. Biochem. Biophys.* **310:**118–125; 1994.
[9] Kaur, H.; Whiteman, M.; Halliwell, B. Peroxynitrite-dependent aromatic hydroxylation and nitration of salicylate and phenylalanine: is hydroxyl radical involved? *Free Radic. Res.* **26:**71–82; 1997.
[10] Wardman, P. Methods to measure the reactivity of peroxynitrite-derived oxidants toward reduced fluoresceins and rhodamines. *Methods Enzymol.* **441:**261–282; 2008.
[11] Lee, J.; Hunt, J. A.; Groves, J. T. Manganese porphyrins as redox-coupled peroxynitrite reductases. *J. Am. Chem. Soc.* **120:**6053–6061; 1998.
[12] Masumoto, H.; Sies, H. The reaction of ebselen with peroxynitrite. *Chem. Res. Toxicol.* **9:**262–267; 1996.
[13] Uppu, R. M.; Winston, G. W.; Pryor, W. A. Reactions of peroxynitrite with aldehydes as probes for the reactive intermediates responsible for biological nitration. *Chem. Res. Toxicol.* **10:**1331–1337; 1997.
[14] Palazzolo-Ballance, A. M.; Suquet, C.; Hurst, J. K. Pathways for intracellular generation of oxidants and tyrosine nitration by a macrophage cell line. *Biochemistry* **46:**7536–7548; 2007.
[15] Pfeiffer, S.; Lass, A.; Schmidt, K.; Mayer, B. Protein tyrosine nitration in cytokine-activated murine macrophages: involvement of a peroxidase/nitrite pathway rather than peroxynitrite. *J. Biol. Chem.* **276:**34051–34058; 2001.
[16] Sampson, J. B.; Ye, Y.; Rosen, H.; Beckman, J. S. Myeloperoxidase and horseradish peroxidase catalyze tyrosine nitration in proteins from nitrite and hydrogen peroxide. *Arch. Biochem. Biophys.* **356:**207–213; 1998.
[17] Miller, E. W.; Chang, C. J. Fluorescent probes for nitric oxide and hydrogen peroxide in cell signaling. *Curr. Opin. Chem. Biol.* **11:**620–625; 2007.
[18] Zhao, W. Lighting up H_2O_2: the molecule that is a "necessary evil" in the cell. *Angew. Chem. Int. Ed. Engl.* **48:**3022–3024; 2009.
[19] Chang, M. C.; Pralle, A.; Isacoff, E. Y.; Chang, C. J. A selective, cell-permeable optical probe for hydrogen peroxide in living cells. *J. Am. Chem. Soc.* **126:**15392–15393; 2004.
[20] Miller, E. W.; Tulyathan, O.; Isacoff, E. Y.; Chang, C. J. Molecular imaging of hydrogen peroxide produced for cell signaling. *Nat. Chem. Biol.* **3:**263–267; 2007.
[21] Kissner, R.; Beckman, J. S.; Koppenol, W. H. Peroxynitrite studied by stopped-flow spectroscopy. *Methods Enzymol.* **301:**342–352; 1999.
[22] Radi, R. Kinetic analysis of reactivity of peroxynitrite with biomolecules. *Methods Enzymol.* **269:**354–366; 1996.
[23] Bonini, M. G.; Augusto, O. Carbon dioxide stimulates the production of thiyl, sulfinyl, and disulfide radical anion from thiol oxidation by peroxynitrite. *J. Biol. Chem.* **276:**9749–9754; 2001.
[24] Lemercier, J. N.; Padmaja, S.; Cueto, R.; Squadrito, G. L.; Uppu, R. M.; Pryor, W. A. Carbon dioxide modulation of hydroxylation and nitration of phenol by peroxynitrite. *Arch. Biochem. Biophys.* **345:**160–170; 1997.
[25] Lymar, S. V.; Jiang, Q.; Hurst, J. K. Mechanism of carbon dioxide-catalyzed oxidation of tyrosine by peroxynitrite. *Biochemistry* **35:**7855–7861; 1996.
[26] Lymar, S. V.; Hurst, J. K. Carbon dioxide: physiological catalyst for peroxynitrite-mediated cellular damage or cellular protectant? *Chem. Res. Toxicol.* **9:**845–850; 1996.
[27] Zhang, H.; Squadrito, G. L.; Pryor, W. A. The mechanism of the peroxynitrite–carbon dioxide reaction probed using tyrosine. *Nitric Oxide* **1:**301–307; 1997.
[28] Keith, W. G.; Powell, R. E. Kinetics of decomposition of peroxynitrous acid. *J. Chem. Soc.* A90; 1969.
[29] LaButti, J. N.; Gates, K. S. Biologically relevant chemical properties of peroxymonophosphate (=O_3POOH). *Bioorg. Med. Chem. Lett.* **19:**218–221; 2009.
[30] Merenyi, G.; Lind, J.; Goldstein, S. The rate of homolysis of adducts of peroxynitrite to the C=O double bond. *J. Am. Chem. Soc.* **124:**40–48; 2002.
[31] DiCesare, N.; Lakowicz, J. R. Chalcone-analogue fluorescent probes for saccharides signaling using the boronic acid group. *Tetrahedron Lett.* **43:**2615–2618; 2002.
[32] Du, L.; Li, M.; Zheng, S.; Wang, B. Rational design of a fluorescent hydrogen peroxide probe based on the umbelliferone fluorophore. *Tetrahedron Lett.* **49:** 3045–3048; 2008.